indices A and B can be completely replaced by the block indices a and b, leaving the formula for the free energy unchanged. However, the interaction parameters are now given by the well-known composition rules

$$\chi_{ab} = (\hat{p}_a - \hat{p}_b)^2\chi_{AB} \quad (A.14)$$

$$\chi_{\kappa a} = \hat{p}_a\chi_{\kappa A} + (1 - \hat{p}_a)\chi_{\kappa B} - \hat{p}_a(1 - \hat{p}_a)\chi_{AB} \quad (A.15)$$

with a similar equation for $\chi_{\kappa b}$ (cf. eq 2.4). That is, a random block can be treated exactly the same way as a normal block if the above effective interaction parameters are used.

References and Notes

(1) Ramos, A. R.; Cohen, R. E. *Polym. Eng. Sci.* **1977**, *17*, 639.
(2) Eastmond, G. C.; Phillips, D. G. *Polymer* **1979**, *20*, 1501.
(3) Riess, G.; Kohler, J.; Tournut, C.; Banderet, A. *Rubber Chem. Technol.* **1969**, *42*, 447.
(4) Krause, S. In "Block and Graft Copolymers"; Burke, J. J., Weiss, V., Eds.; Syracuse University Press: Syracuse, NY, 1973.
(5) Meier, D. J. *Polym. Prepr., Am. Chem. Soc., Div. Polym. Chem.* **1970**, *11*, 400.
(6) Meier, D. J. *Polym. Prepr., Am. Chem. Soc., Div. Polym. Chem.* **1977**, *18*, 340.
(7) Helfand, E. *Macromolecules* **1975**, *8*, 552.
(8) Helfand, E.; Wasserman, Z. R. *Macromolecules* **1980**, *13*, 994.
(9) Leibler, L. *Macromolecules* **1980**, *13*, 1602.
(10) Hong, K. M.; Noolandi, J. *Macromolecules* **1981**, *14*, 727.
(11) Noolandi, J.; Hong, K. M. *Ferroelectrics* **1980**, *30*, 117.
(12) Hong, K. M.; Noolandi, J. *Macromolecules* **1981**, *14*, 1229.
(13) Noolandi, J.; Hong, K. M. *Macromolecules* **1982**, *15*, 482.
(14) Noolandi, J.; Hong, K. M. *Polym. Bull. (Berlin)* **1982**, *7*, 561.
(15) Joanny, J. F.; Leibler, L. *J. Phys. (Orsay, Fr.)* **1978**, *39*, 951.
(16) Roe, R.-J.; Zin, W.-C.; Fishkis, M. Proceedings of IUPAC Meeting, Amherst, MA, July 12–16, 1982, p 662.

Ordered Structure in Block Polymer Solutions. 4. Scaling Rules on Size of Fluctuations with Block Molecular Weight, Concentration, and Temperature in Segregation and Homogeneous Regimes

Takeji Hashimoto,* Mitsuhiro Shibayama, and Hiromichi Kawai

Department of Polymer Chemistry, Faculty of Engineering, Kyoto University, Kyoto 606, Japan.

Received September 17, 1982

ABSTRACT: The small-angle X-ray scattering (SAXS) technique with a position-sensitive detector and a 12-kW rotating-anode X-ray generator was used to study the microdomain size or wavelength of the spatial fluctuations of the A and B segments in AB diblock polymers as a function of the total degree of polymerization of the block polymers (Z), polymer volume concentration (ϕ_P), and temperature (T) in neutral solvents, i.e., solvents good for both A and B block polymers. The block polymers studied were polystyrene–polyisoprene (SI) diblock polymers having about equal block molecular lengths, thus having alternating lamellar microdomains with a lamellar identity period of D in the solutions in the segregation regime. It was found that in the segregation limit D scales as $D/b \sim Z^{2/3}(\phi_P/T)^{1/3}$ or $D/b \sim Z^{1/2}(x/x_c)^{1/3}$, where $x \equiv \phi_P/T$, $x_c \equiv (\phi_P/T)_c$, b is Kuhn's statistical segment length, and $(\phi_P/T)_c$ is the critical value of ϕ_P/T at which the microdomains are dissolved into a homogeneous mixture. At high temperatures ($T > T_c$) or low concentrations ($\phi_P < \phi_c$), the microdomains are dissolved into a homogeneous mixture. The following results were obtained in the homogeneous regime. (i) There exists a scattering maximum, the peak position of which yields the Bragg spacing D. (ii) The scattering can be adequately described in the context of the random phase approximation (RPA) proposed by de Gennes and Leibler. (iii) D satisfies a scaling rule completely different from that obtained for the segregation limit: $D/b \sim Z^{1/2+\beta}(\phi_P/T)^0$ (in the homogeneous regime), where β is related to a small excluded volume effect that exists in the concentrated solutions.

I. Introduction

If two polymers A and B have different cohesive energy densities, they tend to segregate themselves into their respective domains in the segregation limit to result in phase separation. However, due to the *molecular constraint* that A and B chains are covalently bonded in AB or ABA block polymers, the phase separation is restricted to the molecular dimensions, giving rise to *microdomains* whose sizes are controlled by the block molecular weight. This is the phenomenon that is well-known as *microphase separation*.

The physics of flexible, long-chain molecules in such a microdomain system has been extensively explored both theoretically[1-6] and experimentally.[7-10,25] It was borne out that the chains can be essentially described as random flight chains with two important *physical constraints*: (i) *uniform space-filling* with the segments in space and (ii) the *confined volume* effect. The former constraint arises from *incompressibility* of polymeric liquid, the total segment density being kept uniform everywhere in the domain space. The latter constraint arises from the repulsive interactions of the polymers A and B, A (B) chains being likely confined in A (B) domain space.

The degree of the spatial confinement is a function of the effective repulsive potential between the A and B block polymer molecules and hence is a function of temperature and concentration of the polymers if the solvent exists in the system. The theme in this paper and of some of our earlier papers[11-14] is focused on this effect of the degree of the spatial confinement of the chains on the microdomain size or spatial fluctuations of density of the A or B segments in both segregation and homogeneous regimes.

When the temperature is raised above the *thermodynamic transition temperature* (T_c) or the concentration of the polymer is lowered below the *critical concentration* (C_c), the effective repulsive potential or effective Flory–Huggins χ parameter (χ_{eff}) becomes lower than the critical value $\chi_{eff,c}$ required for maintaining the microphase-separated domain structure, resulting in an *order-to-disorder transition*,[11] i.e., the transition involving dissolution of

0024-9297/83/2216-1093$01.50/0

microdomains into a disorderd mixture. The existence of such an order-to-disorder transition was explored both experimentally[11,15-20] and theoretically.[4,6,21,22] In this study we explore the spatial fluctuations of the segmental density in both the ordered state (i.e., the state where the microdomains exist) and the disordered state (i.e., the state where the microdomain is dissolved into a homogeneous mixture) for AB diblock polymers in *neutral solvents*, i.e., solvents good for both A and B polymers.

In part 1[11] of this series we reported the temperature and concentration dependence of the spherical microdomain of polystyrene (PS)–polybutadiene (PB) (SB) diblock polymers in *selective solvents*. We obtained the temperature dependence of the interdomain distance D as

$$D \sim (1/T)^{\sim 1/3} \qquad \text{(I-1)}$$

where T is the absolute temperature. We will show that we can obtain the same temperature dependence for the neutral solvents (see sections III-2 and IV-1). The apparent concentration dependence of D with the neutral solvents will be shown to be completely different from that with the selective solvents (sections III-1 and IV-1).

In part 2[19] of this series, we extensively explored the existence of two transitions, i.e., the *lattice-disordering* and the *order-to-disorder transitions*, of the SB block polymers in selective solvents and some effects of the two transitions on the rheological properties. In part 3[12] we further extended our studies to PS–polyisoprene (PI) (SI) diblock polymer having about equal block molecular length in the neutral solvents. We studied the concentration dependence of the lamellar microdomains at room temperature in the ordered state (i.e., in the segregation regime). In this paper we further extend the studies of the SI diblock polymers in neutral solvents to lower concentrations and higher temperatures and study the spatial fluctuations of the segmental density as a function of total degree of polymerization of the block polymer (Z), polymer volume concentration (ϕ_P), and T.

We describe the experimental conditions in section II, results on concentration dependence in section III-1, and results on temperature dependence in section III-2. On the basis of these results, we derive a scaling rule on D with Z, ϕ_P, and T in the segregation limit in section IV-1 and in the homogeneous limit in section IV-2. We also show that the scattering from the disordered state can be adequately described by a random phase approximation.[22,23] Finally, in section IV-3 we briefly describe equilibrium and nonequilibrium aspects of the lamellar microdomains. This problem will be more extensively discussed in a forthcoming paper (part 5[24]), including spherical microdomains as well.

II. Experimental Technique

PS–PI (SI) diblock polymers, designated as L-2 and L-8, were prepared by a sequential living anionic polymerization. Their total number-average molecular weights were 3.1×10^4 for L-2 and 9.4×10^4 for L-8. Weight fractions of PS were 0.4 and 0.5, respectively. They have different PI microstructures, although the difference is not of much significance in this paper. Polymer L-2 was polymerized in tetrahydrofuran (THF) at −78 °C, thus having high 1,2- and 3,4-addition contents, while polymer L-8 was polymerized in benzene at room temperature, thus having high 1,4-addition content. The Kuhn statistical segment lengths of the PI block chains of L-2 and L-8 are 0.59 and 0.63 nm, respectively.[26,27]

The solution was enclosed in a cell whose details were given in previous papers.[11,12] The small-angle X-ray scattering (SAXS) from solutions was measured at a constant concentration C and temperature T. The solution was heated to about 200 °C, and the temperature was controlled within an accuracy of ±0.5 °C. Toluene and dioctyl phthalate (DOP) were used as neutral solvents, good for both PS and PI. The preparation of toluene solutions and its sampling into the scattering cell were described in detail in the previous paper.[12] There was no trace of solvent leakage from the cell. The temperature dependence of the SAXS profiles can be more easily studied with DOP than with toluene, since DOP is less volatile than toluene. The DOP solutions were prepared by mixing a prescribed amount of SI and the solvent with an excess amount of methylene chloride, which was subsequently completely evaporated to obtain a homogeneous solution of a given concentration.[34]

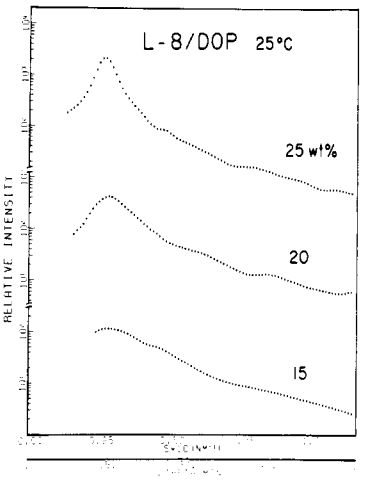

Figure 1. Concentration dependence of SAXS profiles at room temperature for DOP solutions of L-8. $s = (2 \sin \theta)/\lambda$, 2θ being the scattering angle.

The spatial fluctuations of the segmental density in the block polymer solutions were investigated by SAXS as described in detail in the previous papers.[11,12] Unless otherwise stated, the SAXS results were corrected for absorption, background scattering (air scattering, parasitic scattering, and thermal diffuse scattering), nonuniformity of the detector sensitivity, and collimation errors in both the slit-width and slit-length directions according to a method described elsewhere.[28,33]

III. Results

1. Concentration Dependence. The concentration dependence of SAXS profiles was described in detail in part 3[12] for L-8 in toluene solutions in the segregation limit. Here we extended our studies to lower concentrations with DOP solvent. The weak intensity of SAXS at the lower concentrations was detected here for a prolonged counting time. The results are shown in Figure 1, where the corrected scattering profiles at 15, 20, and 25 wt % polymer concentrations are shown. From the peak position ($2\theta_m$) of the SAXS maximum we have evaluated an apparent spacing D by using Bragg's equation

$$2D \sin \theta_m = \lambda \qquad \text{(III-1a)}$$

or

$$s_m = (2 \sin \theta_m)/\lambda = 1/D \qquad \text{(III-1b)}$$

where 2θ is the scattering angle and λ is the wavelength of X-ray, ($\lambda = 0.154$ nm). The results are plotted in Figure 3 with open circles.

The concentration dependence of SAXS profiles was also investigated for the lower molecular weight block

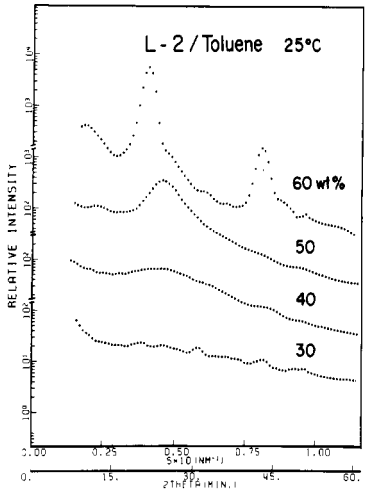

Figure 2. Concentration dependence of SAXS profiles at room temperature for toluene solutions of L-2.

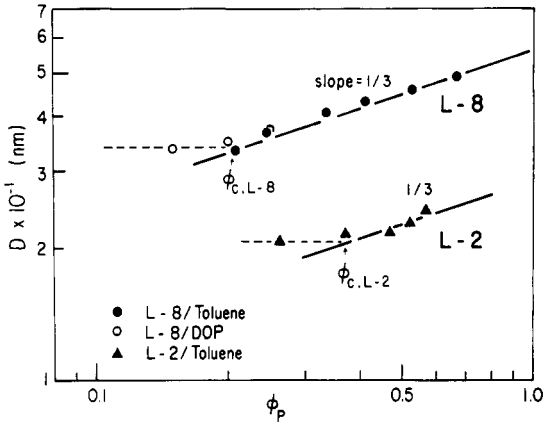

Figure 3. Concentration dependence of the Bragg spacing D at room temperature for L-8 in toluene (solid circles), L-8 in DOP (open circles), and L-2 in toluene (solid triangles). ϕ_P is volume fraction of polymer in solution and ϕ_c is the critical concentration for the order-to-disorder transition.

polymer L-2 in toluene. The results are shown in Figure 2. Comparisons of Figure 3 in ref 12 for L-8 with Figure 2 for L-2 indicate that the critical concentrations at which the first-order maximum and the higher order maxima appear increase with decreasing molecular weight. Thus one can qualitatively conclude that the higher the molecular weight, the lower the critical concentration C_c for the onset of the microphase separation. The concentration C_c is more quantitatively discussed in section IV-2. From the peak position of the SAXS, the value D was estimated by using eq 1, the results of which are plotted in Figure 3.

The solid lines in Figure 3 indicate that the concentration dependence of D is given by

$$D \sim \phi_P^{1/3} \qquad \text{(III-2)}$$

as found in the previous paper[12] (part 3) in the segregation regime. The increase of D with ϕ_P is interpreted in terms of the effect of increasing *segregation power*[11,12] between PS and PI block chains with increasing ϕ_P. In the present work we found a new concentration dependence at the lower concentrations, i.e., the concentration dependence of D being much weaker than that expected from eq III-2 and give approximately by

$$D \sim \phi_P^0 \qquad \text{(III-3)}$$

We tentatively assign this concentration dependence to

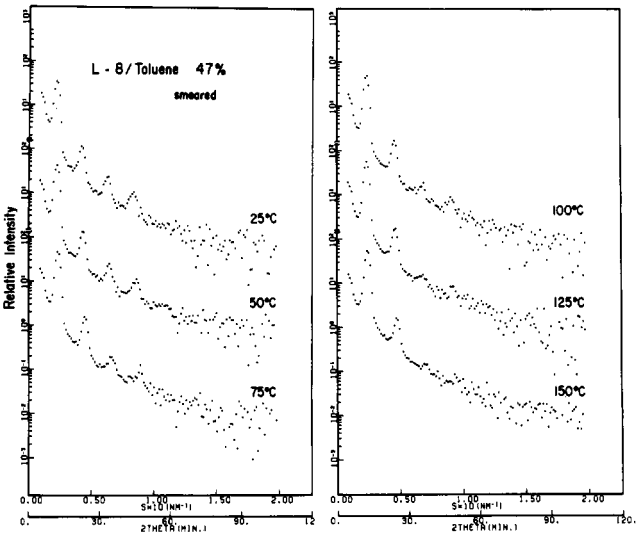

Figure 4. Typical variations of the SAXS profiles with temperature for a 47 wt % toluene solution of L-8.

that characteristic to the disordered state, i.e., to the state where the microdomains are dissolved into a homogeneous mixture. This assignment will be reinforced by the temperature dependence of the SAXS profiles at these concentrations and by the discussion in section IV-2. The *crossover* between the two different concentration dependence, of eq III-2 and III-3 occurs at C_c, the critical concentration for the order-to-disorder transition. One should note that the origin of the scattering maximum in the two regimes is very different, although the spacings in these regimes are quite similar. The maximum in the segregation regime arises from the uniform thickness of each lamella and its spacing, while the maximum in the homogeneous regime arises from the "correlation hole" effect[22,23] in the molecular mixture, as will be described in more detail in section IV-2.

2. Temperature Dependence. We discuss here the temperature dependence of the SAXS profiles in the segregation regime where eq III-2 is applicable. Figure 4 shows typical variation of the SAXS profiles (smeared but corrected for other factors) with temperature for a 47 wt % toluene solution of L-8, where $s = (2 \sin \theta)/\lambda$. At room temperature, a well-developed lamellar microdomain is formed, giving rise to multiple-order scattering maxima at the scattering angles $2\theta_{m,n}$ satisfying

$$2D \sin \theta_{m,n} = n\lambda \qquad \text{(III-4)}$$

where D is again the *lamellar identity period* and n is an integer.

When the temperature is increased, the scattered intensity decreases, the amount of the intensity decay being greater for greater scattering angles, which results in the higest order scattering maximum (the nth maximum) disappearing first at the lowest temperature and then the next highest order maximum ($(n-1)$th maximum) disappearing at a higher temperature. For example, the fourth-order maximum disappears around 125 °C and the third-order maximum disappears around 150 °C. Accompanying the intensity decay with temperature, the peak position $2\theta_{m,n}$ also shifts toward higher angles with increasing temperature.

Such temperature variations of the SAXS profiles as described above, which will be discussed in detail in section IV-1, are a consequence of decreasing segregation power between PS and PI segments with increasing temperature. That is, a decrease in segregation power allows mixing of the unlike segments, which results in an increased *inter-*

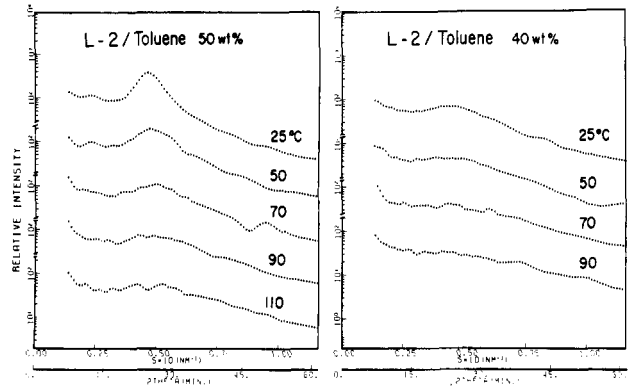

Figure 5. Variations of the SAXS profiles with temperature for 50 and 40 wt % toluene solutions of L-2.

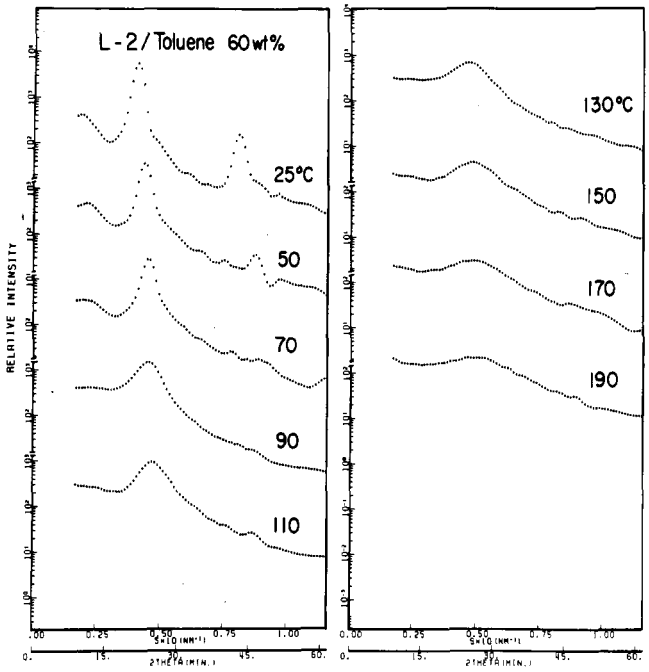

Figure 6. Variations of the SAXS profiles with temperature for a 60 wt % toluene solution of L-2.

facial thickness t of the lamellar microdomains and a decreased D value (see section IV-1). The increased value of t results in the faster decay of the intensity of the higher order scattering maximum than that of the lower order maximum,[35] and the decreased D results in the shift of $2\theta_{m,n}$ toward higher angles with increasing temperature.

Figures 5 and 6 show the temperature variations of the SAXS profiles for 40, 50, and 60 wt % toluene solutions of L-2 specimen, relative intensity being plotted on a logarithmic scale. The temperature variations are similar to those of L-8, showing similar intensity decay and peak shift. It should be noted, however, that for the lower molecular weight material L-2 the higher order scattering maximum disappears at much lower temperature than for the higher molecular weight material L-8 at a given concentration. That is, the unlike segments of the lower molecular weight material are more miscible, having a lower T_c than those of the higher molecular weight material. For a given molecular weight, the lower the concentration, the lower the temperature at which the higher order maxima disappear, i.e., the lower the critical temperature T_c.

It should be noted also that the first-order peak does not easily vanish but persists up to a considerably high temperature as reported by Roe et al.[15] for the SAXS from

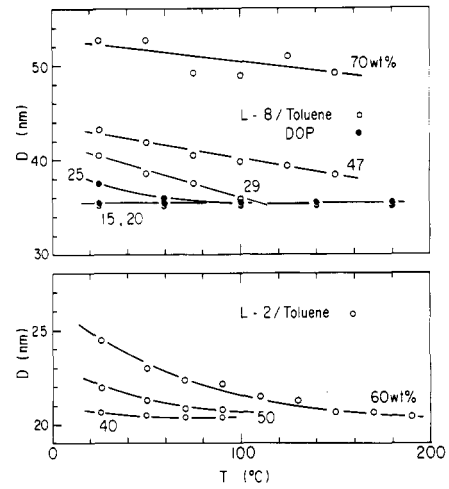

Figure 7. Temperature dependence of the Bragg spacing D for 15, 20, and 25 wt % DOP solutions and 29, 47, and 70 wt % toluene solutions of L-8 and for 40, 50, and 60 wt % toluene solutions of L-2.

bulk block polymers having a lower T_c. It will be clarified in section IV-2 that the SAXS maxima at all the temperatures for the 40 wt % toluene solution of L-2, at temperatures higher than about 90 °C for the 50 wt % toluene solution of L-2, at temperatures higher than about 190 °C for the 60 wt % solution of L-2, at all temperatures for the 15 and 20 wt % DOP solutions of L-8, and at temperatures higher than about 100 °C for the 25 wt % DOP solution of L-8 arise from the fluctuation of the spatial segmental density distribution in the *disordered state* (see Figures 7, 12, and 13).

It may be useful to summarize the variation of the SAXS profiles with temperature at this point. Let us consider the profiles for the 60 wt % solution of L-2 in Figure 6. At low temperature the segregation power is large and a well-defined microdomain structure is formed. When the temperature is increased to about 70 °C, the second-order scattering maximum disappears but the width of the first-order maximum remains essentially unaltered, indicating that the process primarily involves thickening of the domain-boundary interphase,[35] i.e., the mixing of the unlike units in the domain-boundary region being enhanced owing to the decreasing segregation power. Further increase of temperature results in gradual broadening of the first-order maximum and decay of the scattered intensity, as seen in the profiles obtained at 90–190 °C and in those obtained at 25–70 °C for the 50 wt % toluene solution of L-2 (Figure 5). This indicates that the thickness of each lamellar microdomain tends to fluctuate, the fluctuation increasing gradually with increasing temperature, and that the unlike segments are further mixed.

Near the transition temperature, a significant segmental intermixing may take place in each domain as well as in the domain boundary. The fluctuation of the domain size, with overall polymer segmental density constant, and the segmental intermixing may be stabilized by a decrease of the segregation power. The microdomains are eventually dissolved into a disordered mixture at temperatures higher than T_c. Thus this transition of the particular systems we studied here is broad, as claimed by Roe et al.,[15] and is not so sharp as one might expect from the terminology "order-to-disorder transition". The continuous and discontinuous nature of the transition may be further obscured by the fact that even the disordered mixture exhibits the scattering maximum at a scattering angle nearly identical with that for the well-developed microdomains. However, this complication in the transition phenomenon

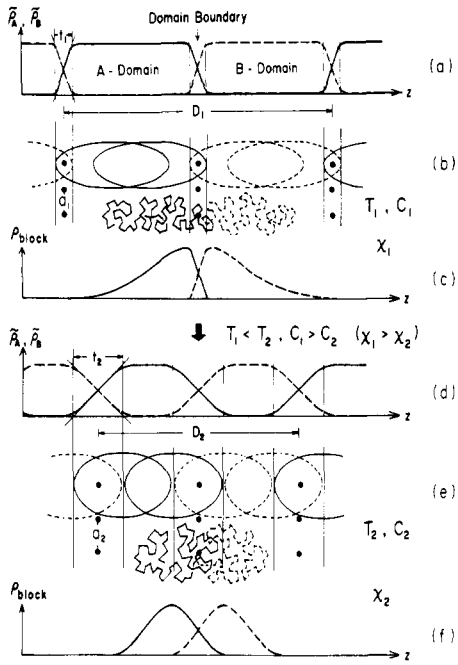

Figure 8. Schematic diagram showing concentration and temperature dependence of the domain size (from D_1 to D_2), average nearest-neighbor distance between the chemical junction points along the interface (from a_1 to a_2), and spatial segmenal density profile of a given block chain.

is an inevitable consequence arising from the *molecular connectivity* of the constituent block chains. We will discuss in section IV-2 a criterion for assessing the transition temperature.

Figure 7 summarizes the temperature and concentration dependence of the identity period of D in the spatial segmental density fluctuations both in the segregation and homogeneous regimes for the L-8 and L-2 specimens. The general trend is that D decreases with increasing temperature and decreasing concentration.[37] For the lower molecular weight block polymer L-2, the value D decreases with increasing T to a constant asymptotic value of about 21 nm which is almost independent of concentrations for the range of the concentrations studied here (40–60 wt %). The same trend is seen for the higher molecular weight block polymer L-8 at lower concentrations (i.e., 15–29 wt %). The constant asymptotic value D, which is about 35 nm, is larger for L-8 than for L-2. For L-8 having concentrations 47 and 70 wt %, the values of D never reach a constant vlue with increasing T, i.e., T_c being much higher than 200 °C at these concentrations.

IV. Discussion

1. Segregation Limit. We will interpret the concentration and temperature dependence of the SAXS profiles from the block polymer solutions in the segregation regime.

In the strong segregation limit, the block chains A and B segregate themselves into their respective microdomains, giving rise to the spatial segmental density proiles $\tilde{\rho}_A$ and $\tilde{\rho}_B$ as shown in Figure 8a, where the microdomains A and B are composed selectively of A and B chains, respectively, and the unlike segments are preferentially mixed only in the domain-boundary region of thickness t_1. Owing to the repulsive interactions between the chains A and B, they are stretched normal to the interface as shown in Figure 8b, where the solid and dashed ellipsoids of revolution stand for the schematically drawn *segmental clouds* of A and B chains, respectively. The segmental cloud of each block chain heavily overlaps those of the neighboring molecules both laterally and longitudinally, giving rise to a uniform overall segmental density everywhere in the domain space.

When temperature is raised or the concentration of the polymer is lowered, the effective repulsive potential between A and B decreases. Now A-block chains tend to have some walks in the B domains, resulting in a thicker domain-boundary thickness t_2 and a smaller end-to-end distance. The smaller end-to-end distance, in turn, results in a smaller domain size and interdomain distance D_2 as shown in Figure 8, parts d and e. The segmental density distribution for a given block chain is skew at lower temperatures and high concentrations, as shown in Figure 8c. It becomes a more symmetric Gaussian-type distribution at high temperatures and low concentrations, as shown in Figure 8f, resulting in an increased conformational entropy of the block chains. Consequently, the increased enthalpy of mixing at the interphase that is caused by decreasing domain size D_2 and hence decreasing surface-to-volume ratio is outweighed and stabilized by the increasing conformational entropy of the A and B chains and the increased entropy of placing the chemical junction points in the interphase, because the interaction parameter between A and B decreases with increasing T. This decrease of the domain size is easily adjusted by the displacement of the chemical junction points along the interface, i.e., by increasing the average distance between the chemical junction points along the interface from a_1 to a_2 as shown in Figure 8, parts b and e.

On the basis of the physical insight gained above, one may think that the domain size D may be primarily determined by the segregation power between the A and B chains in solution, i.e., by the *effective* interaction parameter χ_{eff} between A and B in the presence of the solvent

$$D = D(\chi_{eff}) \qquad \text{(IV-1)}$$

The greater the value χ_{eff}, the larger the value D. The value D depends also on b, the Kuhn statistical segment length. However, the concentration and temperature dependence of b may be much weaker than those of χ_{eff}.

For neutral solvents and at high polymer concentrations, χ_{eff} may be approximated, as in the treatment of Helfand and Tagami,[29] by

$$\chi_{eff} = \chi\phi_P \qquad \text{(IV-2)}$$

where χ is the A–B interaction parameter in bulk. If

$$\chi = A + B/T \simeq B/T \qquad \text{(IV-3)}$$

then it follows that

$$D \simeq D(\phi_P/T) \qquad \text{(IV-4)}$$

If this is the case, the D values measured at various concentrations ϕ_P and temperatures T should fall onto a single *master curve* when the values are plotted as a function of ϕ_P/T.

In Figure 9, the logarithm of D is plotted as a function of the logarithm of ϕ_P/T for the L-2 and L-8 specimens. As expected, a fairly good master relationship was obtained, the data obtained at various concentrations and temperatures falling onto a straight line of slope $^1/_3$. There is a deviation from the straight line for the data points corresponding to the D values of the bulk L-8 at room temperature and those of the Bulk L-2 at temperatures lower than the glass transition temperature of polystyrene. These deviations are obviously associated with the *nonequilibrium effect* encountered in the solvent evaporation process, as discussed in detail in the previous paper[12] and as will be discussed briefly in section IV-3.

If we take into account the molecular weight dependence of the domain size, these two straight lines also may be

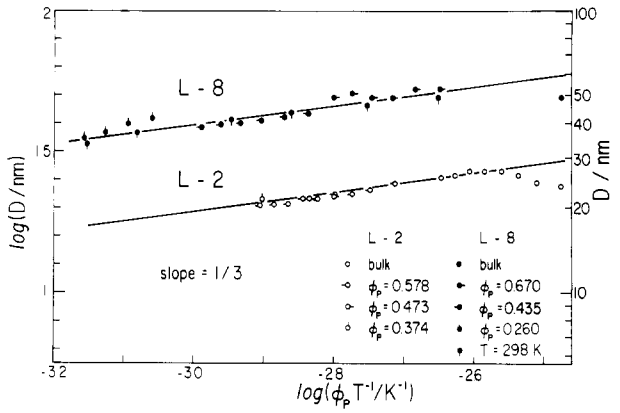

Figure 9. "Master curves" between D and ϕ_P/T for L-2 and L-8.

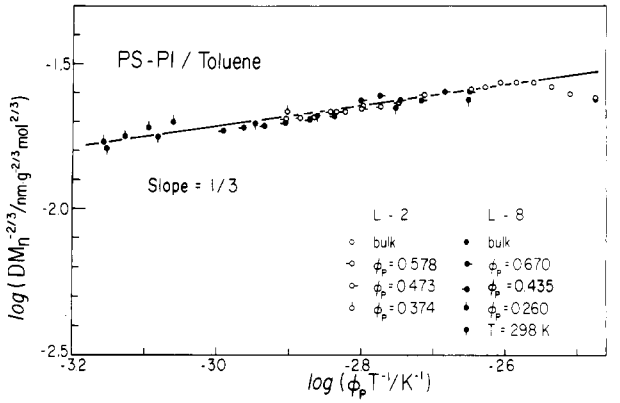

Figure 10. "Master curves" between $D/M_n^{2/3}$ and ϕ_P/T for L-2 and L-8.

superposed on each other by a vertical shift. From our earlier studies[8,9,30] we know that

$$D \sim M_n^{2/3} \text{ or } Z^{2/3} \qquad \text{(IV-5)}$$

where M_n is total molecular weight of the block polymers. Consequently, if D is normalized with $M_n^{2/3}$, then the data points obtained with different molecular weights also should fall onto a single master curve. In fact, as shown in Figure 10 one obtains a *master curve* between log $(D/M_n^{2/3})$ vs. log (ϕ_P/T). Hence

$$D \sim Z^{2/3}(\phi_P/T)^{1/3} \qquad \text{(segregation limit)} \quad \text{(IV-6)}$$

for the ordered state where the microdomains exist in solution.[37]

2. Homogeneous Limit. We consider here the temperature dependence of D in the homogeneous regime ($\phi_P < \phi_c$), where the concentration dependence of D is given by eq III-3. Typical variations of the SAXS profiles with temperature are shown in Figure 5 (40 wt % L-2 solution) and in Figure 11. It should be noted that the peak intensity decays with temperature but the peak position is almost independent of temperature. Thus eq III-3 can be generalized as

$$D \sim (\phi_P/T)^0 \qquad \text{(IV-7)}$$

Moreover, the two horizontal straight lines (broken lines) in Figure 3 can be superposed on each other by a vertical shift, the amount of shift being dependent upon molecular weight, scaling approximately as $M_n^{1/2+\beta}$. Hence,

$$D \sim Z^{1/2+\beta}(\phi_P/T)^0 \qquad \text{(homogeneous limit)} \quad \text{(IV-8)}$$

where β is a small correction factor that depends on the excluded volume effect; β may be nearly zero at the high concentrations covered in this work.

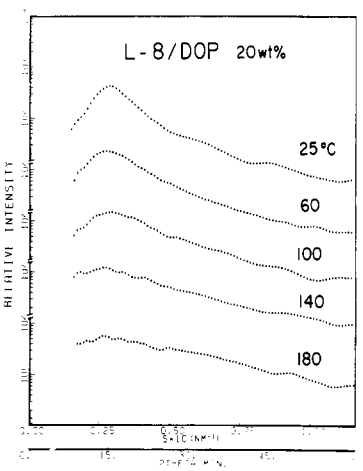

Figure 11. Variations of the SAXS profiles with temperature in the homogeneous limit for a 20 wt % DOP solution of L-8.

Now we must clarify the origin of the SAXS maximum leading to eq IV-8. Intuitively, we think the maximum arises from fluctuations occurring in the disordered state or homogeneous limit where the microdomains are dissolved into the disordered mixture. We will apply the scattering theory from the disordered mixture as proposed by Leibler[22] based upon the random phase approximation.[23] According to Leibler, the scattering intensity $S(q)$ from bulk block polymers in the disordered state is given by

$$S(q) = Z/[F(u) - 2\chi Z] \qquad \text{(IV-9)}$$

where

$$q = (4\pi/\lambda) \sin \theta$$

$$u = q^2R_0^2 \qquad \text{(IV-10)}$$

R_0 is the radius of gyration of the block polymer chain in the bulk. The function $F(u)$ is given by eq IV-6 of ref 22. Equation IV-9 predicts the existence of the scattering maximum. The peak intensity decreases with decreasing χ but the peak position is almost independent of χ, satisfying

$$q_{max} \simeq 1/R_0 \qquad \text{(IV-11)}$$

We may extend Leibler's theory to the concentrated block polymer solutions in the disordered state by replacing χ by χ_{eff} as given by eq IV-2 and by replacing $S(q)$ by $I(q)$

$$I(q) = \phi_P^2 S(q) \qquad \text{(IV-12)}$$

where ϕ_P^2 in eq IV-12 is associated with a decrease of the scattering contrast by addition of the neutral solvents. Then the scattering intensity $I(q)$ from the disordered solution is given by

$$\frac{I(q)}{\phi_P^2} = \frac{Z}{F(u') - 2\chi_{eff}Z} \qquad \text{(IV-13)}$$

where

$$u' = q^2R^2 \qquad \text{(IV-14)}$$

and

$$q_{max} \sim 1/R \qquad \text{(IV-15)}$$

R is the radius of gyration of the block polymer in the concentrated solution. The spacing D calculated from eq IV-15 is thus independent of χ_{eff} and hence of ϕ_P/T from eq IV-2 and IV-3. The value D is proportional to R and hence $Z^{1/2+\beta}$. Thus the theory can justify eq IV-8, and eq

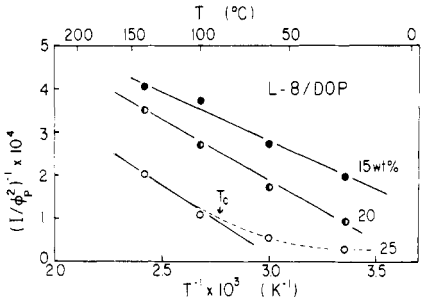

Figure 12. Variations of $(I/\phi_P^2)^{-1}$ with $1/T$ for 15, 20, and 25 wt % DOP solutions of L-8, where I denotes $I(q)$ at $q = q_{max}$ in arbitrary units. T_c stands for the critical temperature.

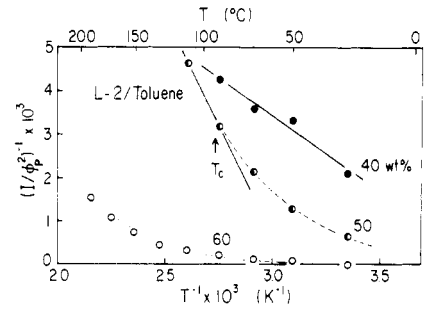

Figure 13. Variations of $(I/\phi_P^2)^{-1}$ with $1/T$ for 40, 50, and 60 wt % toluene solutions of L-2, where I denotes $I(q)$ at $q = q_{max}$ in arbitrary units. T_c stands for the critical temperature.

IV-8 is confirmed to be applicable to the disordered state.

From eq IV-13, one obtains

$$[I(q)/\phi_P^2]^{-1} = F(u')/Z - 2\chi_{eff} \qquad \text{(IV-16)}$$

Substituting eq IV-2 and IV-3 into eq IV-16, one obtains

$$[I(q)/\phi_P^2]^{-1} = (F(u')/Z - 2A\phi_P) - 2B\phi_P/T \qquad \text{(IV-17)}$$

Thus, according to the theory, $(I/\phi_P^2)^{-1}$ should linearly decrease with T^{-1}, the slope of which depends on $B\phi_P$.

The results of testing the theory are shown in Figure 12 for DOP solutions of L-8 and Figure 13 for toluene solutions of L-2. It is obvious that the *linearity* of $(I/\phi_P^2)^{-1}$ with T^{-1} is ensured at low concentrations, e.g., 15 and 20 wt % DOP solutions of L-8 and 40 wt % toluene solutions of L-2. Thus the theory can be justified by experimental results. In the temperature and concentration regimes where the linearity is obtained, the D values are seen to be independent of T and ϕ_P by comparing Figures 12 and 13 with Figure 7. It should be also noted that the slope of the straight line is greater for higher concentrations, consistent with the theoretical prediction of eq IV-17.

At higher concentrations, e.g., 25 wt % DOP solution of L-8 and 50 wt % toluene solution of L-2, linearity is obtained only at high enough temperature, and the deviation from linearity at lower temperatures is considered to be a consequence of *onset* of the microphase separation. For example, for the 25 wt % DOP solution of L-8, the order-to-disorder transition should occur at about $T_c \simeq$ 90 °C, above which linearity is obtained. For the 50 wt % toluene solution of L-2, T_c is nearly equal to 90 °C, and for the 60 wt % toluene solution of L-2, it is equal to or higher than about 190 °C.

Figure 14 summarizes the results. We define x and x_c as

$$x \equiv \phi_P/T \qquad \text{(IV-18a)}$$

$$x_c \equiv (\phi_P/T)_c \qquad \text{(IV-18b)}$$

where x_c is the critical value of x at which the order-to-

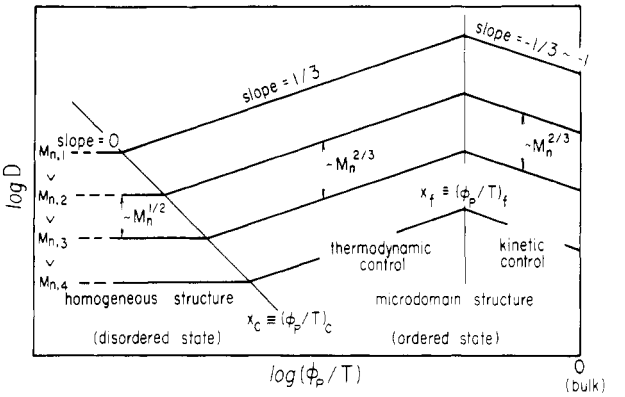

Figure 14. Summary of molecular weight, concentration, and temperature dependence of the domain size D. The variations of log D with log (ϕ_P/T) are plotted for four different molecular weights, $M_{n,1}$ to $M_{n,4}$.

disorder transition occurs. In the regime where $x < x_c$, D is independent of x but dependent upon $M_n^{1/2+\beta}$ or $Z^{1/2+\beta}$, according to eq IV-8. In the regime where $x \geq x_c$, D scales as $x^{1/3}$ and $Z^{2/3}$ or $M_n^{2/3}$. The two regimes correspond, respectively, to the disordered state ($x < x_c$) and ordered state ($x \geq x_c$). The *crossover* occurs at $x = x_c$, whose Z dependence is given as follows. At $x = x_c$ it follows from eq IV-6 and IV-8 that $D \sim Z^{2/3}x_c^{1/3} \sim Z^{1/2+\beta}x_c^0$ and hence

$$x_c \equiv (\phi_P/T)_c \sim Z^{3\beta-1/2} \sim Z^{-1/2} \qquad \text{(IV-19)}$$

Thus the larger the molecular weight, the smaller the value of x_c and consequently the crossover takes place at lower concentrations and higher temperature.

The exponent $-1/2$ is not well understood at this time. It is larger than -1, predicted for the critical point of the ternary mixture of polymer A, polymer B, and solvent in the context of mean field theory[32]

$$(\phi_P/T)_c \sim Z^{-1}$$

The exponent may be modified due to the connectivity between A and B in the block polymers. However, before advancing the arguments, we should note that the exponent $-1/2$ is a tentative value, our experiments being considered to be a preliminary stage for the purpose of assessing the exponent. The accuracy of the exponent $-1/2$ should be much affected by the offset of the chemical compositions of the L-2 and L-8 block polymers as well as the accuracy of the exponents $2/3$ on Z and $1/3$ on ϕ_P/T in eq IV-6 and $1/2 + \beta$ on Z and 0 on ϕ_P/T in eq IV-8. Particularly the assumption of $\beta = 0$ may be crude. Although the general tendency that the larger the molecular weight the smaller the crossover point x_c is correct, the exact assessment of the exponent on Z requires further investigation.

It may be obvious that D is directly proportional to b, Kuhn's statistical segment length. We can summarize eq IV-6 and IV-8 into much simpler form by using the reduced variable x^* as defined by

$$x^* = x/x_c \qquad \text{(IV-20)}$$

That is, from eq IV-6, IV-8, and IV-18 to IV-20, one obtains

$$D/b \sim Z^{1/2}(x^*)^m \qquad \text{(IV-21)}$$

where

$$m = 1/3 \quad \text{for } x^* \geq 1 \quad \text{(segregation limit)} \qquad \text{(IV-22)}$$

$$m = 0 \quad \text{for } x^* < 1 \quad \text{(homogeneous limit)} \qquad \text{(IV-23)}$$

Figure 15 shows a plot of the D value for L-2 and L-8 at various ϕ_P and T as a function of the reduced variable

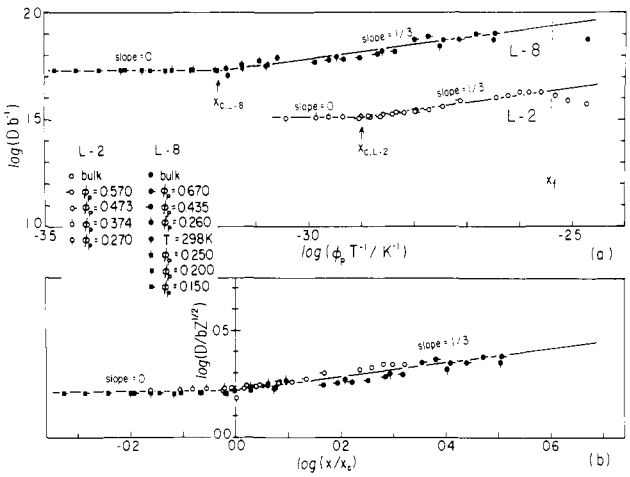

Figure 15. "Master relationships" (a) between D/b and (ϕ_P/T) and (b) between $D/bZ^{1/2}$ and $x^* = x/x_c$, where $x = \phi_P/T$ and $x_c = (\phi_P/T)_c$ (the critical value of x). Note that the data points at $x \geq x_f$ in Figure (a) were neglected in the master curve shown in (b), because they are in the regime of "kinetic control" rather than in the regime of "thermodynamic control".

x^*, where b is the average Kuhn statistical segment length as defined, according to Helfand,[3] by

$$\rho_0 = (\rho_{0S}\rho_{0I})^{1/2} \quad \text{(IV-24)}$$

$$\rho_0 b^2 = (1/2)\rho_{0S} b_S^2 + (1/2)\rho_{0I} b_I^2 \quad \text{(IV-25)}$$

where ρ_{0S} and ρ_{0I} are number density of monomeric units of PS and PI, respectively, and b_S and b_I are the segment lengths of PS and PI, respectively. The degree of polymerization Z of the block polymer was defined as, also according to Helfand,[3]

$$Z = \rho_0[Z_S/\rho_{0S} + Z_I/\rho_{0I}] \quad \text{(IV-26)}$$

where Z_S and Z_I are the degree of polymerization of PS and PI, respectively. As shown in Figure 15 we can obtain a master relationship between $D/bZ^{1/2}$ and x^*.

The crossover point at larger x, i.e., at x_f, will be described in the following section.

3. Equilibrium and Nonequilibrium Aspects of Microdomain Formation. In the preceding sections (sections IV-1 and IV-2) we discussed the effects of the molecular parameters on the *thermodynamically controlled* domain size D or the size of the spatial segmental density fluctuations. Here, we discuss some nonequilibrium effects on D, especially dramatic at high concentrations and at low temperatures, i.e., at $x > x_f$ in Figure 14.

As we discussed in the previous paper (see section IV-2 of ref 12) and in section IV-1 in this paper, the growth of the domain size D with increasing concentration and decreasing temperature involves stretching of the block chains normal to the interface and displacement of the chemical junction points along the interface to reduce the average distance between them. As the concentration is raised, such structural response should be very much slowed down because of either one of the following reasons or of a combination of them as pointed out in the previous paper:[12] as the concentration is raised, (i) the glass transition temperature of the system approaches the ambient temperature and/or (ii) relaxation time for a cooperative deformation of the *grains* increases.[38] It follows eventually at very high concentrations that within a given time scale of the experiment the chemical junction points cannot be rearranged to equilibrium positions, thus the average distance a between the neighboring chemical junction points or the average number of block chains per unit interfacial area being essentially frozen-in. Thus in the regime where $x > x_f$, further evaporation of solvent results in a decrease of the domain size simply by a *deswelling* effect, and the domain size is *kinetically controlled* rather than *thermodynamically controlled*.

The critical concentration x_f may generally depend on molecular weight. However, Figure 14 ignores the molecular weight dependence of x_f for simplicity. The decrease of D with ϕ_P at $x > x_f$ depends on the mechanism of the deswelling, keeping the distance a constant. For isotropic deswelling

$$D \sim \phi_P^{-1/3} \quad \text{(IV-27)}$$

For one-dimensional deswelling in the lamellar microdomains with a fixed distance a

$$D \sim \phi_P^{-1} \quad \text{(IV-28)}$$

For two-dimensional deswelling in the cylindrical microdomains with a fixed distance a

$$D \sim \phi_P^{-1/2} \quad \text{(IV-29)}$$

Acknowledgment. We acknowledge partial financial support from the Ministry of Education, Science and Culture, Japan, under Grants 56490013 addressed to T.H.

Registry No. Isoprene–styrene copolymer, 25038-32-8.

References and Notes

(1) Meier, D. J. *J. Polym. Sci., Part C* **1969**, *26*, 81.
(2) Meier, D. J. *Prepr. Polym. Colloq., Soc. Polym. Sci., Jpn., Kyoto* **1977**, 83.
(3) Helfand, E. *Macromolecules* **1975**, *8*, 552.
(4) Helfand, E.; Wasserman, Z. R. *Macromolecules* **1976**, *9*, 879; **1978**, *11*, 960; **1980**, *13*, 994.
(5) Hong, K. M.; Noolandi, J. *Macromolecules* **1980**, *13*, 964; **1981**, *14*, 727, 736.
(6) Noolandi, J.; Hong, K. M. *Ferroelectrics* **1980**, *30*, 117.
(7) Hashimoto, T.; Todo, A.; Itoi, H.; Kawai, H. *Macromolecules* **1977**, *10*, 377.
(8) Hashimoto, T.; Shibayama, M.; Kawai, H. *Macromolecules* **1980**, *13*, 1237.
(9) Hashimoto, T.; Fujimura, M.; Kawai, H. *Macromolecules* **1980**, *13*, 1660.
(10) Hashimoto, T.; Shibayama, M.; Fujimura, M.; Kawai, H. *Mem. Fac. Eng. Kyoto Univ.* **1981**, *43* (2), 184.
(11) Shibayama, M.; Hashimoto, T.; Kawai, H. *Macromolecules* **1983**, *16*, 16 (part 1 of this series).
(12) Shibayama, M.; Hashimoto, T.; Hasegawa, H.; Kawai, H. *Macromolecules*, in press (part 3 of this series).
(13) Hashimoto, T.; Shibayama, M.; Kawai, H. *Polym. Prepr., Am. Chem. Soc., Div. Polym. Chem.* **1982**, *23* (1), 21.
(14) Hashimoto, T. Proceedings of the IUPAC 28th Macromolecular Symposium, University of Massachusetts, Amherst, MA, 1982, p 705.
(15) Roe, R. J.; Fishkis, M.; Chang, C. J. *Macromolecules* **1981**, *14*, 1091.
(16) Widmaier, J. M.; Meyer, G. C. *J. Polym. Sci., Polym. Phys. Ed.* **1980**, *18*, 2217.
(17) Watanabe, H.; Kotaka, T.; Hashimoto, T.; Shibayama, M.; Kawai, H. *J. Rheol.* **1982**, *26* (2), 153.
(18) Kraus, G.; Hashimoto, T. *J. Appl. Polym. Sci.* **1982**, *27*, 1745.
(19) Hashimoto, T.; Shibayama, M.; Kawai, H.; Watanabe, H.; Kotaka, T. *Macromolecules* **1983**, *16*, 361 (part 2 of this series).
(20) Hashimoto, T.; Tsukahara, Y.; Kawai, H. *J. Polym. Sci., Polym. Lett. Ed.* **1980**, *18*, 585; *Macromolecules* **1981**, *14*, 708.
(21) Meier, D. J. *Org. Coat. Plast. Chem.* **1977**, *37* (1), 246.
(22) Leiber, L. *Macromolecules* **1980**, *13*, 1602.
(23) See, for example: de Gennes, P. G. "Scaling Concepts in Polymer Physics"; Cornell University Press: Ithaca, NY, 1979; Chapter IX.
(24) Shibayama, M.; Hashimoto, T.; Kawai, H. *Macromolecules*, in press (part 5 of this series).
(25) Hadziioannou, G.; Skoulios, A. *Macromolecules* **1982**, *15*, 258, 271.
(26) Hashimoto, T.; Nakamura, N.; Shibayama, M.; Izumi, A.; Kawai, H. *J. Macromol. Sci., Phys.* **1980**, *B17* (3), 389.
(27) Brandrup, J.; Immergut, E. H., Eds. "Polymer Handbook"; Wiley: New York, 1975.
(28) Fujimura, M.; Hashimoto, T.; Kawai, H. *Mem. Fac. Eng., Kyoto Univ.* **1981**, *43* (2), 224.
(29) Helfand, E.; Tagami, Y. *J. Chem. Phys.* **1972**, *56*, 3592.

(30) Equation IV-5 is applicable also to cylindrical microdomains.[31]
(31) Mori, K.; Hasegawa, H.; Hashimoto, T.; Kawai, H., to be submitted to *Macromolecules*.
(32) Scott, R. L. *J. Chem. Phys.* **1949**, *17*, 279.
(33) Todo, A.; Hashimoto, T.; Kawai, H. *J. Appl. Crystallogr.* **1978**, *11*, 558.
(34) It was pointed out by a reviewer that the presence of methylene chloride could lower the vapor pressure of the DOP and allow substantial evaporation of the DOP as the methylene chloride is removed. Although the DOP concentration levels in the systems were not studied by an independent means in this work, one may have to bear in mind this effect for more quantitative studies.
(35) It should be noted in Figure 4 that the widths of the first-order and second-order peaks remain essentially constant with increasing temperature, despite the fact that the higher order peaks (the third- and fourth-order peaks) disappear with increasing temperature. This fact strongly suggests that the disappearance of the higher order peaks with increasing temperature is due to the increasing interfacial thickness but not to the disordering of the lattice structure or the smallness of the grain structure within which the orientation of lamellae is coherent, as is the case in the wide-angle X-ray diffraction. The effect of the interfactial thickness on the SAXS profile is given by

$$I(s;\sigma) = I(s;\sigma=0) \exp(-4\pi^2\sigma^2 s^2)$$

where σ is the parameter characterizing the thickness of the diffuse interphase and $I(s;\sigma=0)$ is the scattered intensity for the system having zero interfacial thickness. Thus the greater the scattering angle, the larger the intensity decay due to the finite interfacial thickness σ.[7,24,36]
(36) Hashimoto, T.; Kowsaka, K.; Shibayama, M.; Kawai, H., to be submitted to *Macromolecules*; *Polym. Prepr., Am. Chem. Soc., Div. Polym. Chem.* **1983**, *24* (2).
(37) It should be noted that an effect of thermal expansion should increase the domain size and domain identity period D with increasing temperature. However, this effect is trivial and much outweighed by the effect of segregation power. The effect of the different thermal expansion coefficients in both phases in the phase-separated systems may vary the scattering contrast, affecting the scattered intensity. However, this effect is again much outweighed by the effect of the segregation power.
(38) The "grain" refers to a region in wich the orientation of the lamellar microdomains is coherent. Increasing segregation power accompanied by increasing concentration involves deformation of the grain in such a way that its dimension normal to the interface should expand but the dimensions parallel to it shrink.

Microphase Structure of Solvent-Cast Diblock Copolymers and Copolymer–Homopolymer Blends Containing Spherical Microdomains

Frank S. Bates,† C. V. Berney, and R. E. Cohen*

Department of Chemical Engineering, Massachusetts Institute of Technology, Cambridge, Massachusetts 02139. *Received October 27, 1982*

ABSTRACT: Investigated in this work were the effects of solvent-casting conditions, the presence of homopolymer in the continuous phase, and the magnitude of block molecular weights on the structural features of styrene–butadiene diblock copolymers and diblock copolymer–homopolystyrene blends containing spherical domains of polybutadiene. Domain boundary thickness, domain size, and domain packing order were determined from small-angle neutron scattering (SANS) measurements. Domain boundary thickness was essentially identical for all samples and in agreement with theory. Contrary to theory, sphere radius was found to be proportional to the 0.37 power of polybutadiene molecular weight; this is shown to be an artifact of the solvent-casting process. Under equilibrium conditions, the domains form a body-centered-cubic paracrystalline macrolattice which is disrupted by the addition of homopolystyrene.

Introduction

Block copolymer structure and properties have generated considerable scientific interest over the past 2 decades. Recent years have found significant advances made in the study of morphology, in large part due to the growing popularity of small-angle scattering techniques. Hashimoto et al.[1–6] have been particularly active in this area, examining polystyrene–vinylpolyisoprene diblock copolymers containing lamellar and spherical (rubber) microdomains by small-angle X-ray scattering (SAXS). Their results leave several unanswered questions with respect to the spherical morphology. For example, these authors found the domain radius to be almost half that predicted from theory,[7] which they contend is a result of the process of solvent casting. Also, no specific domain packing order could be clearly established for their samples.

The present paper is part of a larger study designed to examine relationships between microphase structure and mechanical behavior in block copolymers and polymer blends. Five polystyrene–polybutadiene diblock copolymers and seven diblock copolymer–homopolystyrene blends have been prepared, three of these containing perdeuterated polybutadiene and all exhibiting a morphology consisting of polybutadiene microspherical domains.

The structural features of these materials have been investigated by small-angle neutron scattering (SANS), exploiting the enhanced contrast that results from the use of deuterated butadiene. We presently report on the domain order, domain size (also determined by electron microscopy), and domain boundary thickness in solvent-cast films; homopolystyrene content and block molecular weights are the major variables of the study. SANS determination of the polybutadiene block single-chain behavior has been reported separately.[8] The dynamic mechanical properties of these materials and their relationship to the presently detailed structures are reported in the accompanying paper immediately following this one.

Experimental Section

Materials. Styrene monomer (Aldrich Chemical Co.) was deinhibited by washing with 10% NaOH followed by distilled water and was stored over CaH_2 at 0 °C. Prior to use, the styrene was distilled and redistilled from fresh Na wire and used within 2 h.

1,3-Butadiene (Matheson, high purity) was deinhibited with a 10% NaOH solution, dried over NaOH pellets and molecular

† Present address: Bell Laboratories, Murray Hill, NJ 07974.

0024-9297/83/2216-1101$01.50/0